DOI: 10.17344/acsi.2024.8791 *Acta Chim. Slov.* **2024,** *71,* 528–539

Scientific paper

Synthesis of (*E*)-3-{[2-Oxo-5-arylfuran-3(2*H*)-ylidene] methyl}-4*H*-1-benzopyran-4-ones, Crystal Structure, Quantum Chemical Substantiation

Ekaterina M. Arzyamova*, Olga A. Mazhukina and Alevtina Yu. Yegorova

Institute of Chemistry, N. G. Chernyshevsky Saratov National Research State University, 83 Ulitsa Astrakhanskaya, 410012 Saratov, Russia.

** Corresponding author: E-mail: katerina285@yandex.ru Tel.: +7 9873122099*

Received: 00-00-2024

Abstract

A directed method for the preparation of hybrid compounds based on furan-2(3*H*)-ones and chromen-4(4*H*)-one, (*E*)-3-{[2-oxo-5-arylfuran-3(2*H*)-ylidene]methyl}-4*H*-1-benzopyran-4-ones, the structure of which was confirmed by elemental analysis, IR, UV, NMR spectroscopy, and X-ray single crystal analysis, was developed. The molecular geometry of the synthesized compound (*E*)-3-((2-oxo-5-phenylfuran-3(2*H*)-ylidene)methyl)-4*H*-chromen-4-one (**3a**) was analyzed and compared with X-ray diffraction data, DFT calculations were performed using 6-311G split-valence basis functions.

Keywords: Synthesis; hybrid structures; furan-2(3*H*)-ones; chromen-4(4*H*)-ones; crystal structure; DFT.

1. Introduction

Furan-2(3*H*)-one derivatives are among a large number of compounds with antinociceptive, anti-inflammatory, antiviral and antitumor activities.[1–4] It is important to note nitrofuran derivatives with pronounced antibacterial activity.[5–9] The 4*H*-chromen-4-one fragment is part of the structure of compounds with anticancer, antibacterial, antiviral and other activities[10–12] (Figure 1).

The main focus of this study is the synthesis of hybrid molecules based on furan-2(3*H*)-ones and 4-oxo-4*H*-chromen-3-carbaldehyde. Despite the large number of works on the synthesis of hybrid molecules based on

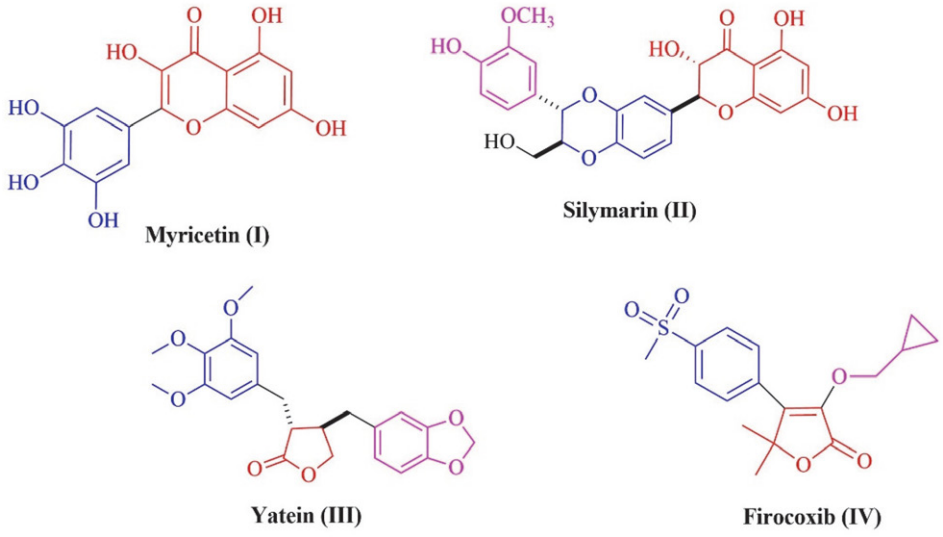

Figure 1. Examples of naturally occurring biologically active hybrid molecules

chromen-4-ones and furan-2-ones, systematic studies of directly coupled 4*H*-chromen-4-ones and furan-2(3*H*)-ones are very limited. The literature review showed that the construction of hybrid molecules is based on reactions with furan-2(5*H*)-one derivatives.[13–17] The only example of the synthesis of hybrid structures based on 4*H*-chromen-4-ones and furan-2(3*H*)-ones, which are intermediates in the synthesis of 4,4-diaryl-1-(3-chromonyl)buta-1,3-dien-2-carboxylic acids **4**, was described by A. K. El-Ziaty *et al.*[18] Condensation of 4-oxo-4*H*-chromen-3-carboxaldehyde **2** with 3-aroylpropionic acids **1** under harsh conditions using thionyl chloride in *N*,*N*-dimethylformamide as a cyclodehydrating agent leads to the formation of the corresponding 5-aryl-3-chromonylmethylene-2(3*H*)-furanones **3** as a mixture of (*E*) and (*Z*) stereoisomers.[18]

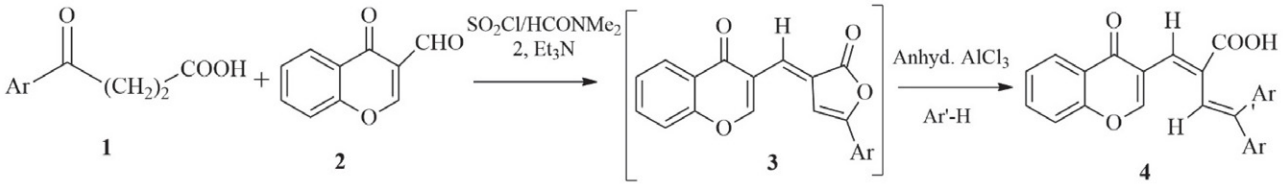

Scheme 1. The synthetic route for compounds **4**

The main disadvantages of this method of synthesis are that it is a multistage, labor intensive process with a long duration, as well as the difficulty of separating products obtained in the form of an inseparable mixture of isomers with low yields. No convincing proof of the structures of the obtained compounds on the basis of the present spectral data was given. The methodology developed by the authors[18] for the synthesis of 5-aryl-3-chromonylmethylene-2(3*H*)-furanones **3** is not reproducible.

Thus, the present work is devoted to finding optimal synthesis conditions and revealing the features of the spatial structure and configuration of hybrid structures: (*E*)-3-{[2-oxo-5-arylfuran-3(2*H*)-ylidene]methyl}-4*H*-1-benzopyran-4-ones.

2. Experimental

2. 1. Materials

The reactions were carried out using Monowave 50 (Anton Paar, Austria) reactor. FTIR spectra were collected on an FSM-1201 Fourier spectrometer (Infraspek, St. Petersburg, Russia) in the range 4000–400 cm^{-1} with a spectral resolution of 4 cm^{-1}. Samples were mixed with ground KBr (FTIR grade, Sigma–Aldrich, Saint Louis, MO, USA) and pressed into pellets by removing water and air traces under reduced pressure. UV spectra of the studied solutions were recorded on a Shimadzu-1800 spectrophotometer in cuvettes with an optical layer thickness of 1 cm and a scanning step of 1 nm. Working solutions were prepared according to the exact weight of the compounds and dissolved in chloroform, ethanol and DMSO ($c = 2 \cdot 10^{-5}$ M). ^{1}H (400 MHz) and ^{13}C NMR (100 MHz), ^{1}H–^{13}C gHSQC, ^{1}H–^{13}C gHMBC, NOESY 2D, NOESY 1D spectra in DMSO-d_6 were recorded with a Varian (Agilent) 400 spectrometer (Agilent Technologies, Santa Clara, CA, USA), and the internal standard was TMS. Chemical shifts (δ) are reported in ppm. Elemental analysis was done on an Elementar Vario MICRO cube CHNS analyzer (Elementar Analysensysteme GmbH, Hanau, Germany). Melting points were determined on a Stuart™ SMP10 melting point apparatus (Cole-Parmer, Beacon Road, Stone, Staffordshire, ST15 OSA, UK). The progress of the reaction and the purity of the synthesized compounds were monitored by TLC on ALUGRAM® SIL G UV254 plates (Macherey-Nagel GmbH & Co. KG, Düren, Germany), with hexane–ethyl acetate–acetone (3:1:1) as the eluent.

2. 2. Quantum Chemical Calculations

Quantum chemical calculations were performed using density functional theory (DFT) using the hybrid functional Lee–Yang–Parr three-parameter Becke B3LYP, split-valence basis set functions 6–311G, with the inclusion of p-orbitals of the hydrogen atom and d-orbitals for more heavy atoms as well as with the addition of polarization functions (B3LYP/6–311G++ (d,p)). For each of the possible isomers, a complete geometry optimization was carried out with a strict convergence criterion.[19]

2. 3. Synthesis of the Compounds

General methodology for the preparation of hybrid structures 3a-f

Method A: A mixture of 3 mmol of the corresponding 5-arylfuran-2(3*H*)-ones **1a–f**, 3 mmol of 4-oxo-4*H*-chromen-3-carboxaldehyde **2** was refluxed in 10 mL of glacial acetic acid. The precipitated yellow crystals were filtered, washed with glacial acetic acid, recrystallized from benzene, and dried.

Method B: The 1 mmol of the corresponding 5-arylfuran-2(3*H*)-one **1a–f**, 1 mmol of 4-oxo-4*H*-chromene-3-carboxaldehyde **2** and 3.5 mL of glacial acetic acid are placed in a 10 mL borosilicate glass vial, placed in the vial with the reaction mixture with a magnetic stirrer. The vial is hermetically sealed with a silicone stopper and placed in a Monowave 50 reactor. The reaction is carried out at a temperature of 135 °C with a stirring speed of 600 rpm.

The precipitated yellow crystals were filtered, washed with glacial acetic acid, recrystallized from benzene, and dried.

(*E*)-3-((2-Oxo-5-phenylfuran-3(2*H*)-ylidene)methyl)-4*H*-chromen-4-one (3a).

Yellow crystals (benzene): *Method A* – 0.66 g, yield 70%; *Method B* – 0.25 g, yield 80%, mp 219–220 °C; FTIR (KBr) ν/cm^{-1}: 1759 (O–C=O), 1653 (C=O), 1613 (C=C); ^{1}H NMR (400 MHz, DMSO-d_6): δ 9.09 (s, 1H, C–H$_{Chromone}$), 8.15 (d, *J* = 8.0 Hz, 1H, Ar–H), 7.89–7.82 (m, 3H, Ar–H), 7.75 (d, *J* = 8.0 Hz, 1H, Ar–H), 7.59 (s, 1H, C–H$_{Furanone}$), 7.56–7.49 (m, 4H, Ar–H), 7.38 (s, 1H, =CH–); ^{13}C NMR (100 MHz, DMSO-d_6): δ 175.06 (C=O), 168.76 (O–C=O), 159.43 (C–H$_{Chromone}$), 156.19, 155.92, 155.86, 135.40, 131.18, 129.57, 128.12, 126.79, 126.09, 125.69, 125.37, 125.31, 125.27 (=CH–), 123.46, 119.79, 119.15, 102.35 (C–H$_{Furanone}$). Anal. calcd. for $C_{20}H_{12}O_4$: C, 75.94; H, 3.82. Found: C, 76.35; H, 4.14%.

(*E*)-3-((2-Oxo-5-(*para*-tolyl)furan-3(2*H*)-ylidene) methyl)-4*H*-chromen-4-one (3b).

Yellow crystals (benzene): *Method A* – 0.52 g, yield 52%; *Method* B – 0.22 g, yield 66%, mp 243–245 °C; FTIR (KBr) ν/cm^{-1}: 1760 (O–C=O), 1646 (C=O), 1615 (C=C); ^{1}H NMR (400 MHz, DMSO-d_6): δ 9.09 (s, 1H, C–H$_{Chromone}$), 8.15 (d, *J* = 8.0 Hz, 1H, Ar–H), 7.88 (t, *J* = 7.0 Hz, 1H, Ar–H), 7.77–7.72 (m, 3H, Ar–H), 7.58–7.53 (m, 2H, Ar–H and C–H$_{Furanone}$), 7.34 (d, *J* = 8.0 Hz, 3H, 2H Ar–H and =CH–), 2.36 (s, 3H, CH$_3$); ^{13}C NMR (100 MHz, DMSO-d_6): δ 175.09 (C=O), 168.86 (O–C=O), 159.24 (C–H$_{Chromone}$), 156.45, 155.92, 141.32, 135.40, 130.50, 130.19, 126.78, 126.09, 125.70, 125.39, 125.33, 124.57 (=CH–), 123.44, 123.39, 119.83, 119.16, 101.50 (C–H$_{Furanone}$), 21.58 (CH$_3$). Anal. calcd. for $C_{21}H_{14}O_4$: C, 76.35; H, 4.27. Found: C, 76.80; H, 4.41%.

(*E*)-3-((5-(4-Chlorophenyl)-2-oxofuran-3(2*H*)-ylidene) methyl)-4*H*-chromen-4-one (3c).

Yellow crystals (benzene): *Method A* – 0.58 g, yield 55%; *Method* B – 0.22 g, yield 63%, mp 284–285 °C; FTIR (KBr) ν/cm^{-1}: 1757 (O–C=O), 1649 (C=O), 1615 (C=C); ^{1}H NMR (400 MHz, DMSO-d_6): δ 9.10 (s, 1H, C–H$_{Chromone}$), 8.16 (d, *J* = 8.0 Hz, 1H, Ar–H), 7.90–7.83 (m, 3H, Ar–H), 7.77 (d, *J* = 8.2 Hz, 1H, Ar–H), 7.66 (s, 1H, C–H$_{Furanone}$), 7.66–7.59 (m, 2H, Ar–H), 7.56 (d, *J* = 7.0 Hz, 1H, Ar–H), 7.41 (s, 1H, =CH–); ^{13}C NMR (100 MHz, DMSO-d_6): δ 175.22 (C=O), 168.75 (O–C=O), 159.03 (C–H$_{Chromone}$), 157.37, 156.29, 155.13, 154.93, 135.53, 129.77, 127.52, 127.40, 126.78, 126.11, 126.02 (=CH–), 125.97, 125.09, 123.35, 119.25, 119.19, 103.09 (C–H$_{Furanone}$). Anal. calcd. for $C_{20}H_{11}ClO_4$: C, 68.49; H, 3.16; Cl, 10.11. Found: C, 68.54; H, 3.35; Cl, 10.20%.

(*E*)-3-((5-(4-Bromophenyl)-2-oxofuran-3(2*H*)-ylidene) methyl)-*4H*-chromen-4-one (3d).

Yellow crystals (benzene): *Method A* – 0.97 g, yield 82%; *Method B* – 0.36 g, yield 90%, mp 271–272 °C; FTIR (KBr) ν/cm^{-1}: 1755 (O–C=O), 1649 (C=O), 1614 (C=C); ^{1}H NMR (400 MHz, DMSO-d_6): δ 9.09 (s, 1H, C–H$_{Chromone}$), 8.16 (d, *J* = 8.0 Hz, 1H, Ar–H), 7.88 (t, *J* = 7.0 Hz, 1H, Ar–H), 7.79–7.74 (m, 5H, Ar–H), 7.67 (s, 1H, C–H$_{Furanone}$), 7.57 (t, *J* = 7.6 Hz, 1H, Ar–H), 7.42 (s, 1H, =CH–); ^{13}C NMR (100 MHz, DMSO-d_6): δ 175.24 (C=O), 168.40 (O–C=O), 157.07 (C–H$_{Chromone}$), 156.31, 155.91, 155.28, 154.45, 134.70, 132.66, 127.61, 127.54, 126.84, 126.10, 125.98 (=CH–), 124.52, 124.09, 123.46, 119.76, 119.18, 103.16 (C–H$_{Furanone}$). Anal. calcd. for $C_{20}H_{11}BrO_4$: C, 60.78; H, 2.81; Br, 20.22. Found: C, 60.54; H, 2.98; Br, 20.09%.

(*E*)-3-((5-(3,4-Dimethylphenyl)-2-oxofuran-3(2*H*)-ylidene)methyl)-4*H*-chromen-4-one (3e).

Yellow crystals (benzene): *Method A* – 0.59 g, yield 57%; *Method* B – 0.23 g, yield 68%, mp 232–233 °C; FTIR (KBr) ν/cm^{-1}: 1761 (O–C=O), 1651 (C=O), 1612 (C=C); ^{1}H NMR (400 MHz, DMSO-d_6): δ 9.08 (s, 1H, C–H$_{Chromone}$), 8.15 (d, *J* = 8.0 Hz, 1H, Ar–H), 7.87 (t, *J* = 7.0 Hz, 1H, Ar–H), 7.75 (d, *J* = 8.4 Hz, 1H, Ar–H), 7.62 (s, 1H, Ar–H), 7.56 (t, *J* = 8.1 Hz, 2H, Ar–H), 7.50 (s, 1H, C–H$_{Furanone}$), 7.34 (s, 1H, =CH–), 7.29 (d, *J* = 8.0 Hz, 1H, Ar–H), 2.27 (unresolved singlet, 6H, 2CH$_3$); ^{13}C NMR (100 MHz, DMSO-d_6): δ 175.09 (C=O), 168.90 (O–C=O), 159.16 (C–H$_{Chromone}$), 156.61, 155.92, 140.22, 137.65, 135.38, 130.65, 126.76, 126.58, 126.09, 125.68, 125.38, 124.34, 124.31 (=CH–), 123.31, 119.84, 119.15, 101.33 (C–H$_{Furanone}$), 19.96 (CH$_3$), 19.82 (CH$_3$). Anal. calcd. for $C_{22}H_{16}O_4$: C, 76.73; H, 4.68. Found: C, 76.97; H, 4.86%.

(*E*)-3-((5-(4-Methoxyphenyl)-2-oxofuran-3(2*H*)-ylidene)methyl)-4*H*-chromen-4-one (3f).

Yellow crystals (benzene): *Method A* – 0.51 g, yield 49%; *Method* B – 0.21 g, yield 60%, mp 241–242 °C; FTIR (KBr) ν/cm^{-1}: 1764 (O–C=O), 1653 (C=O), 1614 (C=C); ^{1}H NMR (400 MHz, DMSO-d_6): δ 9.06 (s, 1H, C–H$_{Chromone}$), 8.15 (d, *J* = 8.0 Hz, 1H, Ar–H), 7.87 (t, *J* = 8.7 Hz, 1H, Ar–H), 7.79–7.74 (m, 3H, Ar-H), 7.54 (t, *J* = 8.1 Hz, 1H, Ar–H), 7.44 (s, 1H, C–H$_{Furanone}$), 7.31 (s, 1H, =CH–), 7.09 (d, *J* = 8.8 Hz, 2H, Ar–H), 3.82 (s, 3H, OCH$_3$); ^{13}C NMR (100 MHz, DMSO-d_6): δ 175.11 (C=O), 168.97 (O–C=O), 158.89 (C–H$_{Chromone}$), 156.46, 155.93, 135.36, 130.23, 129.39, 127.59, 126.73, 126.25, 126.09, 125.44, 124.70, 123.42 (=CH–), 120.57, 119.91, 119.15, 115.17, 100.24 (C–H$_{Furanone}$), 55.94 (OCH$_3$). Anal. calcd. for $C_{21}H_{14}O_5$: C, 72.83; H, 4.07: Found: C, 72.99; H, 4.32%.

2. 4. Single Crystal X-ray Crystallography

The X-ray diffraction study of (*E*)-3-((2-oxo-5-phenylfuran-3(2*H*)-ylidene)methyl)-4*H*-chromen-4-one (**3a**) was performed on an Agilent New Xcalibur, Ruby diffractometer equipped with a CCD detector (MoKα radiation, λ = 0.71073 Å, graphite monochromator, ω-scan) at 295(2)

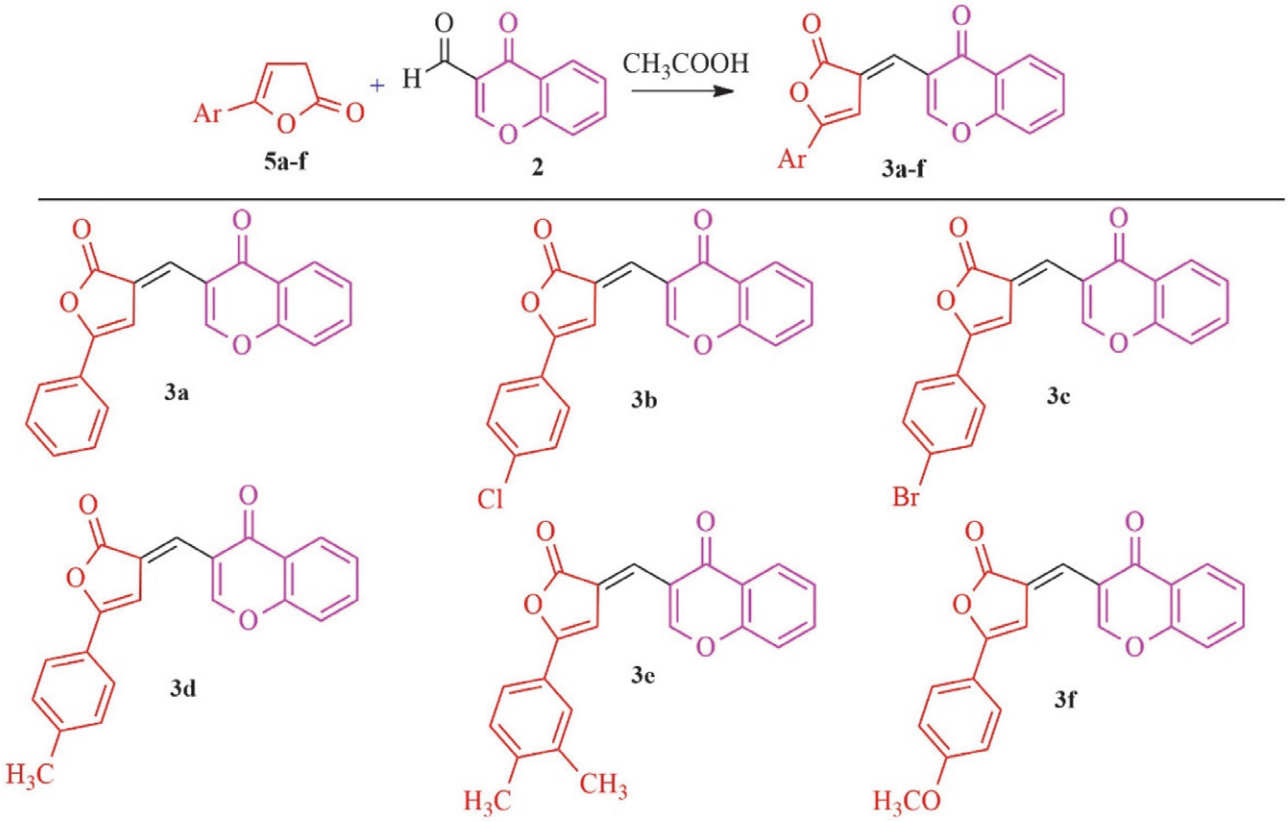

Scheme 2. Synthesis of hybrid structures: 3-{[2-oxo-5-arylfuran-3(2*H*)-ylidene]methyl}-4*H*-1-benzopyran-4-ones **3**

Table 1. Crystallographic data and refinement parameters for the compound **3a**.

Crystal data	
Chemical formula	$C_{20}H_{12}O_4$
M_r	316.30
T/K	295
Crystal system, space group	Monoclinic, $P2_1$
a/Å	6.802(2)
b/Å	4.9703(16)
c/Å	22.217(9)
α/°	90
β/°	92.46(3)
γ/°	90
V/ Å^3	750.4(4)
Z	2
D_{calc} / g cm^{-3}	1.400
μ/mm^{-1}	0.10
F(000)	328
Reflections collected	2103
Independent reflections	2103
$I \geq 2_\sigma(I)$	973
R_{int}	0.037
$R[I \geq 2\sigma(I)]$	0.051
S	0.85
wR(I)	0.116
No. of parameters	218
No. of restraints	1
$\Delta\rho_{min}/\Delta\rho_{max}$ (eÅ^{-3})	–0.16/0.14

K. Absorption corrections were made using CrysAlis PRO program (Agilent Technologies) version 1.171.42.74a. Empirical corrections for absorption were made using spherical harmonics implemented in the SCALE3 ABSPACK program.[20] The structure was refined by full-matrix MNC on F^2 in the anisotropic approximation for all non-hydrogen atoms using the SHELXL program[21] with the OLEX2 graphical interface.[22] The hydrogen atoms of the aromatic rings are refined in a "riding" model. The other hydrogen atoms are included in the refinement independently in the isotropic approximation. The crystal refined as a two-component twin with component occupancies of 0.564(2) and 0.436(2), respectively. Component 2 rotated by –179.9940° around [0.00 0.00 1.00] (reciprocal) or [0.16 0.00 0.99] (direct).

3. Results and Discussion

As a result of the search for optimal conditions for the synthesis of arylmethylidene derivatives, we expanded the series and found the optimal method for the preparation of 3-{[2-oxo-5-arylfuran-3(2*H*)-ylidene]methyl}-4*H*-1-benzopyran-4-ones **3a**–**f** , based on the reaction of equimolar amounts of 5-arylfuran-2(3*H*)-ones **5a**–**f**, obtained according to the method,[23] with 4-oxo-4*H*-chromene-3-carboxaldehyde (**2**) in glacial acetic acid without the use of a

catalyst (Scheme 2), with thermal activation of the reaction mixture and the use of a Monowave 50 closed-type reactor with various yields (Table 2). Considering the presence of three electrophilic centers in 3-formylchromone, several directions of reactions can be expected. Taking into account the structure of (*E*)-3-{[2-oxo-5-arylfuran-3(2*H*)-ylidene]methyl}-4*H*-1-benzopyran-4-ones **3a–f**, it is assumed that the initial enolization of the furanone ring in acetic acid occurs followed by the formation of a new C=C bond due to the involvement of the aldehyde group of substrate **2** in the reaction.

A comparison was made of two interaction methods: the conventional method of thermal heating under normal pressure conditions and in a closed vessel reactor (Monowave 50) at elevated pressure. The use of a sealed vessel reactor makes it possible to increase the efficiency of the process by increasing the temperature and pressure of the reaction, which will significantly reduce its time, which is unattainable under normal conditions of conventional heating at atmospheric pressure and the boiling point of the solvent. The parameters of the two modes are presented in Table 2.

It was shown that the reaction of 5-arylfuran-2 (3*H*)-ones **5a–f** with 3-formylchromone **2**, carried out both under conventional conditions and in a sealed vessel reactor, leads to (*E*)-3-{[2-oxo -5-arylfuran-3(2*H*)-ylidene] methyl}-4*H*-1-benzopyran-4-ones **3a–f**. It should be noted that the use of a reactor in a sealed vessels made it possible to increase the yield of products by 8–14%, as well as significantly increase the efficiency of interaction, which is reflected in a significant reduction in reaction time compared to conventional conditions (12 times) and compared to the literature data (20 times).[18]

The structure of hybrid compounds **3a-f** was confirmed by IR, ^{1}H, ^{13}C NMR, NOESY spectroscopy, and X-ray diffraction analysis using the example of (*E*)-3-((2-oxo-5-phenylfuran-3(2*H*)-ylidene)methyl)-4*H*-chromen-4-one **3a**. The IR spectra of the obtained compounds contain absorption bands of the lactam carbonyl group in the region of 1764–1755 cm^{-1}, as well as absorption bands of the carbonyl group of the 4*H*-chromen-4-one fragment at 1653–1646 cm^{-1}.

The key signals of (*E*)-3-{[2-oxo-5-arylfuran-3(2*H*)-ylidene]methyl}-4*H*-1-benzopyran-4-ones **3a–f** registered in DMSO-d_6 are the proton singlet chromen-4-one fragment at 9.06–9.10 ppm, singlet of the vinyl proton of the furan-2-one fragment at 7.44–7.67 ppm and a singlet of the vinyl proton of the exocyclic bond at 7.31–7.42 ppm. In the low-field region of the ^{13}C NMR spectra of compounds **3a–f**, signals of the lactone carbon atom were recorded at 168.40–168.97 ppm and the carbonyl carbon atom of the chromen-4-one fragment at 175.06–175.24 ppm.

Based on NMR spectroscopy, it was shown that the resulting compounds **3a–f** exist only in the form of *E*-isomers. Proof of this is the absence of duplication of signals in the ^{1}H NMR spectra, recorded in DMSO-d_6, as well as the presence in the NOESY 2D spectra of the example of compound **3a** of a cross-peak at 7.59/9.09 ppm, due to the NOE correlation of the proton at the C–4 position of furan-2-one fragment and the proton of the C-2 position of the chromen-4-one fragment (Figure 2), both in general form and upon selective excitation within the NOESY 1D method, which confirms their closeness and indicates in favor of the *E*-configuration. Additional confirmation is the absence of NOE correlation between the vinyl proton of the exocyclic bond and the vinyl proton of the furan-2-one fragment.

Figure 2. Key NOE correlation for (*E*)-3-((2-oxo-5-phenylfuran-3(2*H*)-ylidene)methyl)-4*H*-chromen-4-one **3**a

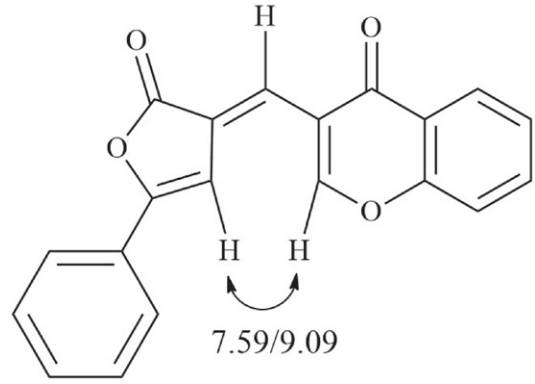

The synthesized compounds **3a–f**, regardless of the reaction conditions, exist in a DMSO-d_6 solution only in the *E*-configuration. To identify the features of the spatial structure, reaction direction and configuration of the re-

Table 2. Optimal conditions for the synthesis of hybrid structures **3a-f**.

№	Reflux				Monowave 50			
	T, °C	*t*, min	*P*, bar	Yield, %	*T*, °C	*t*, min	*P*, bar	Yield, %
3a	118	180	1	70	135	15	4	80
3b	118	180	1	52	135	15	4	66
3c	118	60	1	55	135	5	4	63
3d	118	60	1	82	135	5	4	90
3e	118	180	1	57	135	15	4	68
3f	118	180	1	49	135	15	4	60

sulting hybrid structures **3a–f**, their theoretical study was carried out based on DFT calculations.[19]

It is known that M-base-catalyzed condensation reactions produce a chelate transition state, first proposed by Zinmerman, which has a chair conformation. This hypothesis perfectly explains the possibility of obtaining a stereoselective result. It is possible to unambiguously establish the direction of transformation only in the case of intramolecular transformations.

The intermolecular nature of reactions makes it impossible to unambiguously determine the location of the reacting substances. Under the proposed conditions, in the acid-catalyzed transformation, enolization occurs due to protonation of the carbonyl group of the furan-2-one moiety, which leads to the formation of a planar cyclic conjugated system. Subsequent attack by the activated carbonyl group on the chromenonaldehyde can occur from opposite sides relative to the ring plane and ultimately leads to the formation of four possible isomeric aldols *R*1, *R*2 and *S*1, *S*2 (Scheme 3).

According to the calculated molecular geometry data, the *R*1 isomer is stabilized due to the formation of an intramolecular hydrogen bond, as a result of which the formation energy of this aldol is less important compared to other isomers (Figure 3).

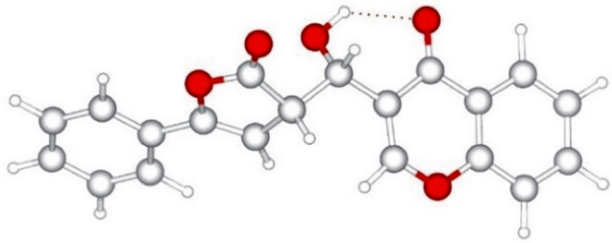

Figure 3. Optimized structure of compound **3a** (isomer *R*1)

The final product of the transformation in the process under study is 3-((2-oxo-5-phenylfuran-3(2*H*)-ylidene) methyl)-4*H*-chromen-4-one (**3a**), which can exist in the form of four geometric isomers *E*1, *E*2 , *Z*1, *Z*2 (Scheme 4).

This result is due to the different mutual arrangement of groups of atoms of the chromenone fragment due to its rotation around a single C–C bond within a fixed geometric configuration. According to calculated data, the probability of the formation of the *R*1 isomer is higher; subsequent dehydration processes will lead to one of the *E* forms. According to NMR spectroscopy data (the presence of a corresponding cross-peak in the NOESY 2D and NOESY 1D spectra) and the results of X-ray diffraction studies, we have a single *E*1 isomer as the final product of the reaction.

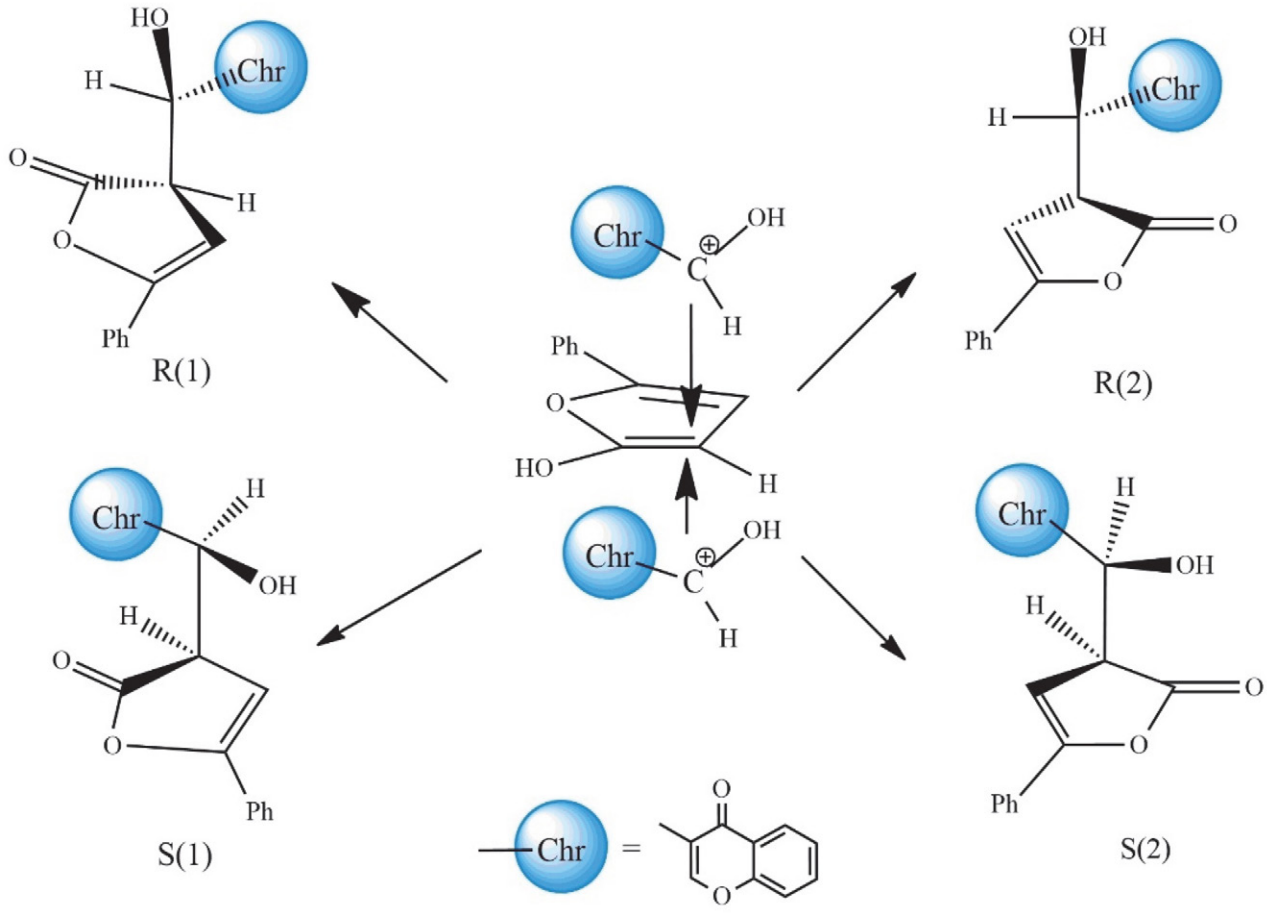

Scheme 3. Formation of possible isomeric aldols *R*1, *R*2, *S*1, *S*2

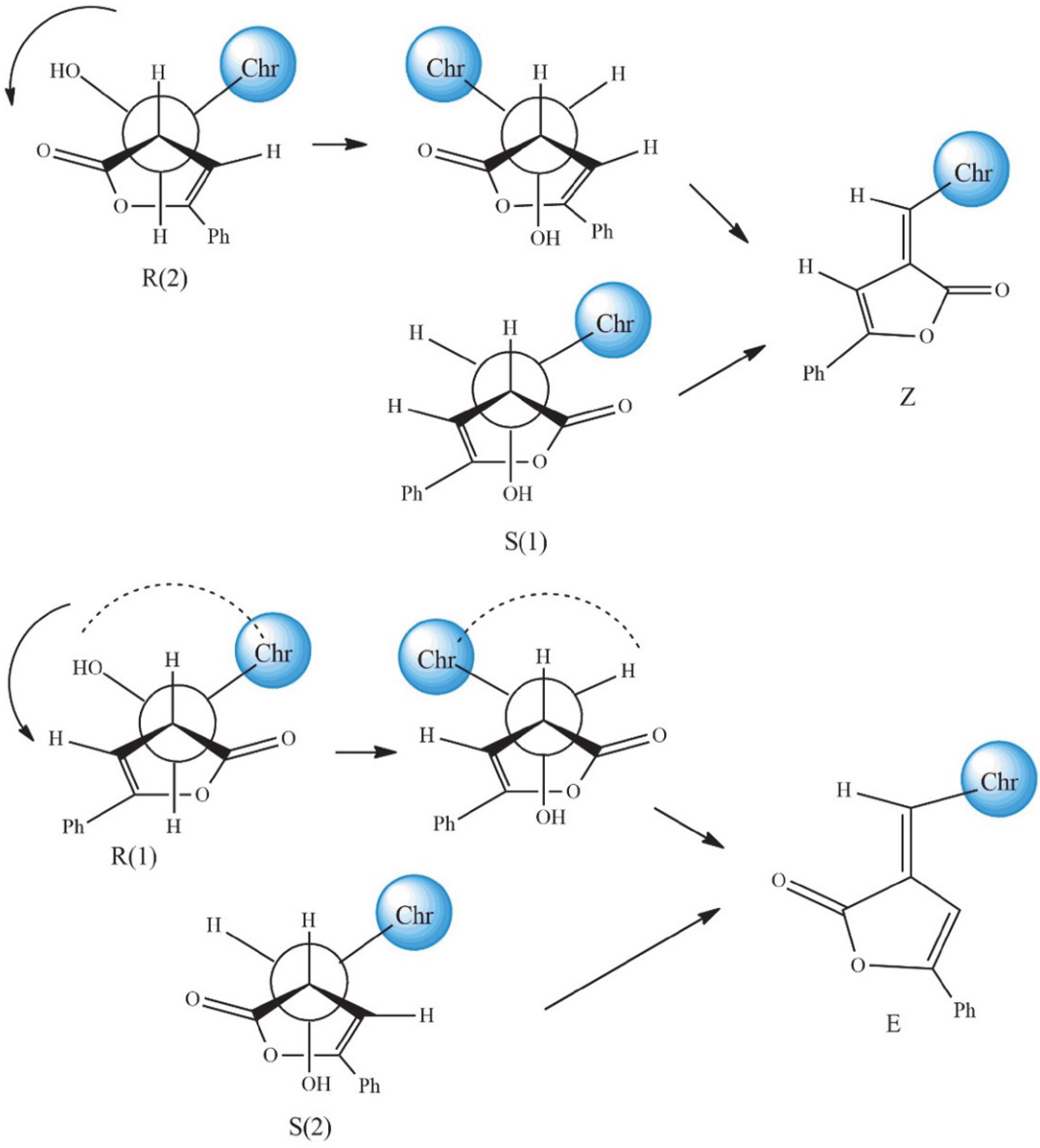

Scheme 4. Geometric isomers *E*1, *E*2, *Z*1, *Z*2 of 3-((2-oxo-5-phenylfuran-3(2*H*)-ylidene)methyl)-4*H*-chromen-4-one (**3a**)

A suitable crystal of compound **3a** was grown by slowly cooling a saturated solution in benzene. For X-ray diffraction analysis, a crystal with a size of 0.6 × 0.1 × 0.02 mm^3 was selected. The crystal structure of compound **3a** with atom labeling is shown in Figure 4. From this experiment, we were able to further confirm that the final compounds **3a**–**f** are in the *E*1 configuration. (*E*)-3-((2-oxo-5-phenylfuran-3(2*H*)-ylidene)methyl)-4*H*-chromen-4-one (**3a**) crystallizes in the non-centrosymmetric space group $P2_1$ with one molecule in the independent part of the unit cell.

The crystal packing for (*E*)-3-((2-oxo-5-phenylfuran-3(2*H*)-ylidene)methyl)-4*H*-chromen-4-one (**3a**) is shown in Figure 5, according to which the minimum

Table 3. Geometric parameters of (*E*)-3-((2-oxo-5-phenylfuran-3(2*H*)-ylidene)methyl)-4*H*-chromen-4-one (**3a**) according to X-ray diffraction results.

Angle	(°)	Bond lengths	(Å)
C11–C12–C16	117.2	C11–C12	1.44
C11–C12-C13	121.6	C12–C13	1.36
C3–C11–C12	131.6	C12–C16	1.44
C4–C3–C11	121.6	C3–C2	1.49
C12–C13–H13	118.4	C2–H2	0.93
C13–C12–C11–C3	14.7	C11–H11	0.93
C12–C11–C3–C2	7.4	C13–H13	0.93
H11–C11–C12–C16	9.3		
C11–C12–C13–H13	–6.6		
C4–C3–C11–C12	–174.1		

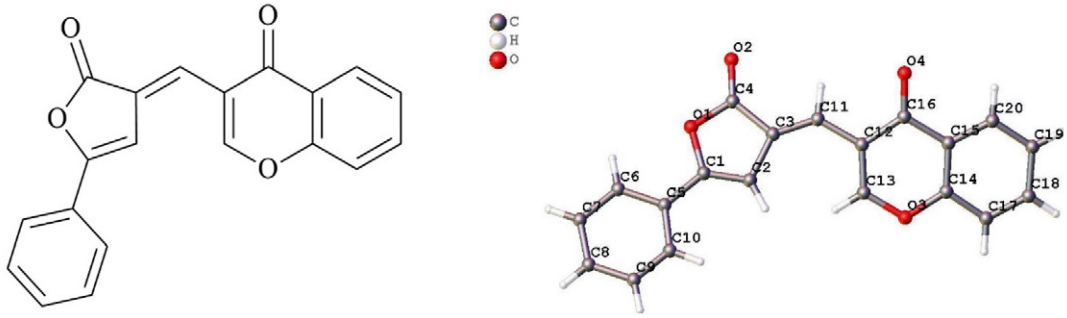

Figure 4. General view of compound **3a** in the representation of atoms by thermal ellipsoids (p = 50%).

distance between two molecules oriented parallel to each other is 4.97 Å, which indicates the absence of effective intermolecular interaction of the stacking type.

The phenyl substituent practically lies in the same plane with the furan-2(3*H*)-one ring, the angle between the C2–C1–O1–C4–C3 and C5–C6–C7–C8–C9–C10 planes is 6.8°. The chromenone fragment is rotated relative to the furan-2(3*H*)-one ring in such a way that the angle between the C2–C1–O1–C4–C3 and C17–C18–C19–C20–C15–C14 planes is 21.1°. The C5–C6–C7–C8–C9–C10 planes of the phenyl substituent and the C17–C18–C19–C20–C15–C14 planes of the chromenone ring are located at an angle of 28.8°.

We carried out a theoretical justification for the configurational features of the obtained series of compounds based on DFT calculations. For this purpose, the B3LYP functional and the 6–31G(d,p) basis set were used.

Using compound **3a** as an example, the geometry of all 4 possible configurations (*E*1, *E*2, *Z*1, *Z*2) was optimized (Table 4). The first parameter that demonstrates the correlation of the resulting structure with the *E*1 form is the angle between the planes C14–C11–C10–O9–C5–C4–C3–C2–C7–C6–C5 of phenylmethylenefuranone and C15–C16–O17–C18–C21–C22–C23–C24–C19–C20 of chromenone fragments, which is 23.7° and corresponds to that in X-ray diffraction analysis (25.01°); the

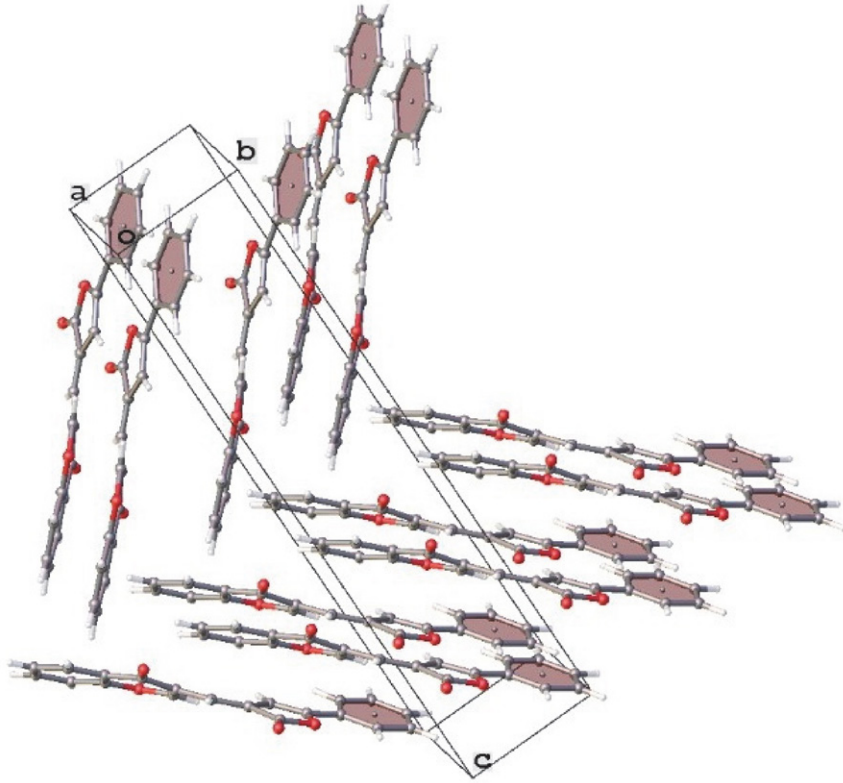

Figure 5. The packing diagram of compound **3a**

distance between the centers of the indicated planes of the structures under consideration is 7.43 Å and 7.45 Å, respectively. A confirming factor is also the close distance between the H33–H31 hydrogen atoms, equal to 2.18 Å in the *E*1 structure with optimized geometry (Figure 6) and 2.11 Å, respectively, in the crystal of the resulting substance.

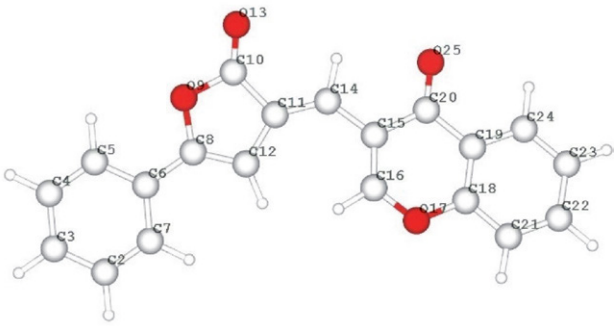

Figure 6. Optimized structure of compound **3a** (*E*1 isomer)

When comparing the values of bond angles in the calculated model of configuration *E*1 with the values obtained from X-ray diffraction studies, it can also be noted that they are almost identical. The values of the torsion angles differ, which is explained by the different rotation angle of the chromenone cycle plane relative to the phenylmethylenefuranium plane (Figure 7).

A comparative analysis of the experimentally obtained and theoretically calculated ^{1}H NMR spectra (Table 5) is also consistent with the above, with the exception of the shift of the vinyl proton of the furanone ring to a weaker field compared to that of the exocyclic fragment.

Table 5. Key signals of ^{1}H NMR spectra of optimized isomer structures *E*1, *E*2, *Z*1, *Z*2 of compound **3***a*.

Key signals	3a				
	Experiment	Calculation			
		***E*1**	***E*2**	***Z*1**	***Z*2**
$CH_{furanone}$	7.59	7.25	8.89	7.19	7.09
=CH–	7.37	8.11	7.31	8.39	7.39
$CH_{Chromone}$	9.09	9.03	8.75	11.29	8.57

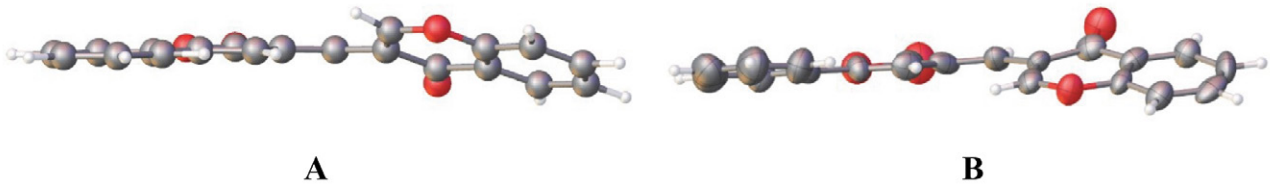

A **B**

Figure 7. The location of the chromenone ring relative to the phenylmethylenefuranone ring in the optimized *E*1 molecule (**A**) and in the crystal according to X-ray diffraction analysis (**B**)

Table 4. Geometric parameters of the optimized structures of isomers *E*1, *E*2, *Z*1, *Z*2 of compound **3a**.

	Compound			
	3a (E1)	**3a (E2)**	**3a (*Z*1)**	**3a (*Z*2)**
Bond lengths (Å)				
C14–C15	1.45	1.45	1.45	1.46
C15–C16	1.36	1.37	1.37	1.35
C15–C20	1.48	1.48	1.49	1.48
C11–C12	1.44	1.44	1.44	1.44
C12–H31	1.08	1.07	1.08	1.08
C14–H32	1.09	1.09	1.09	1.09
C16–H33	1.08	1.08	1.08	1.08
Angle (°)				
C14–C15–C20	117.2	126.4	115.2	174.9
C14–C15–C16	123.9	115.6	125.9	119.2
C11–C14–C15	129.5	134.1	134.5	126.9
C10–C11–C14	119.8	117.2	129.7	125.9
C15–C16–H33	124.1	122.6	123.5	123.4
C16–C15–C14–C11	–22.2	179.98	0	139.22
C15–C14–C11–C12	–3.8	0.02	–0.004	172.9
H32–C14–C15–C20	–16.7	179.97	0	131.4
C14–C15–C16–H33	–1.5	–0.001	0	–2.5
C10–C11–C14–C15	177.7	–179.99	0	–11.8

If we consider the parameters of the theoretical model of the *E*2 isomer (*Z*1, *Z*2), then almost all the lengths of the compared bonds will coincide with those for the experimentally obtained one from X-ray diffraction analysis data. However, the values of the bond and torsion angles will differ. In addition, based on these values of torsion angles for isomeric structures, we can conclude that *E*2 is almost flat, and this configuration is stabilized due to an intramolecular hydrogen bond (O25–H31) 2.17 Å, which illustrates an even greater shift to the downfield region of the vinyl proton of furan-2-one ring.

Like the theoretical model *E*2, its isomer *Z*1 is planar and stabilized by a hydrogen bond (O13–H33) of 2.01 Å, which contributes to a shift in the calculated spectrum to the region of 11.29 ppm vinyl proton of the chromenone ring.

In contrast to the latter, the model of isomer *Z*2 has an even larger angle between the phenylmethylene-furanone and chromenone planes (C14–C11–C10–O9–C5–C4–C6–C3–C2–C7 and C15–C16–O17–C18–C21–C22–C23–C24–C19–C20) and amounts to 49.7°, due to repulsion between exocyclic oxygen atoms - oxygen of the furanone and chromenone rings.

Thus, a comparative analysis of data from theoretical calculations of geometry (distances, bond and torsion angles) and spectral data with data obtained from X-ray diffraction and spectral analyzes clearly shows the unambiguity of the formation of the *E*1 stereoisomer. The obtained results of calculating the geometry and energy parameters of the intermediates of the condensation process (*R* and *S* adducts) make it possible to explain the further direction of the process of formation of stereoisomer *E*, as a product of dehydration of the most stable *R*1 isomer.

We also discovered the ability of 3-{[2-oxo-5-arylfuran-3(2*H*)-ylidene]methyl}-4*H*-1-benzopyran-4-ones **3a**–**f** to exist only in one *E*-configuration by electron spectroscopy. For compounds **3a**, **3c**, **3f**, containing electron-donating and electron-withdrawing substituents and having different chromophores, electronic absorption spectra were recorded in various solvents ($c = 2 \cdot 10^{-5}$ M) and various pH values. Regardless of the polarity of the chosen solvent and the structure of the aromatic sub-

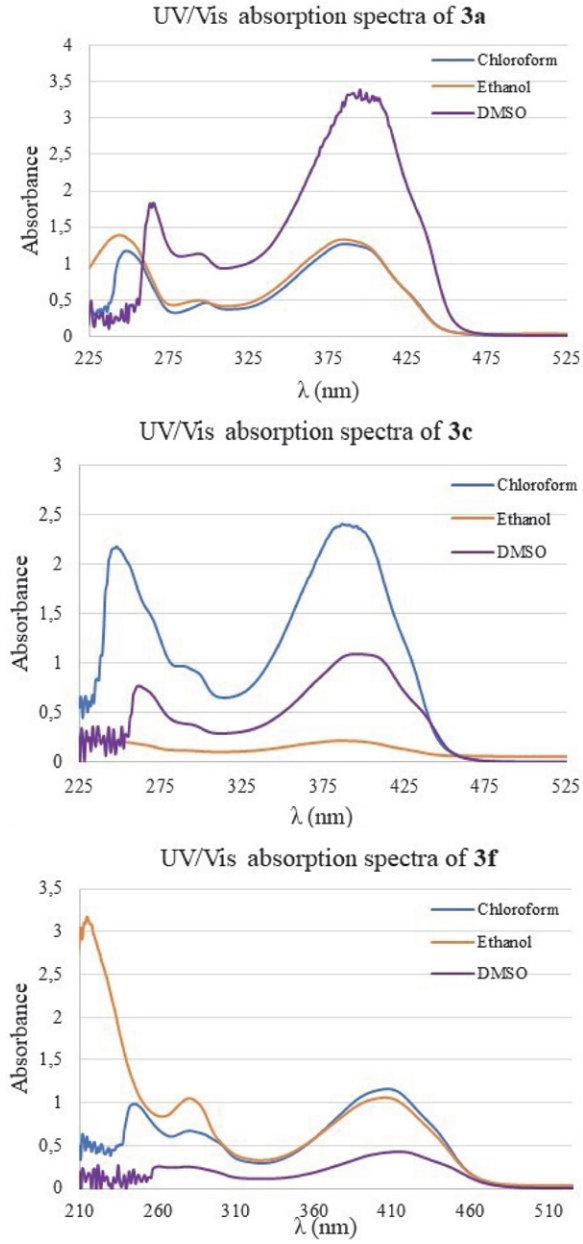

Figure 8. UV/Vis absorption spectra of **3a**, **3c**, **3f** in $CHCl_3$, EtOH, DMSO

Table 6. Characteristics of 3-{[2-oxo-5-arylfuran-3(2*H*)-ylidene]methyl}-4*H*-1-benzopyran-4-ones **3a**, **3c**, **3f** in solvents of various polarities in neutral and acidic media.

№	λ_{max}, nm (A)					
	$CHCl_3$	$CHCl_3 + CH_3COOH$	EtOH	EtOH + CH_3COOH	DMSO	DMSO + CH_3COOH
3a	248 (1.18)	248 (1.22)	244 (1.39)	246 (1.60)	—	—
	298 (0.45)	298 (0.48)	294 (0.49)	294 (0.57)	294 (1.13)	294 (1.24)
	386 (1.24)	388 (1.27)	384 (1.33)	385 (1.58)	403 (3.30)	404 (3.40)
3c	248 (2.17)	248 (2.19)	241(0.21)	229 (1.41)	—	—
	288 (0.97)	288 (0.99)	298 (0.11)	299 (0.44)	296 (0.37)	295 (0.44)
	391 (2.39)	392 (2.40)	393 (0.21)	391 (0.68)	396 (1.09)	400 (1.18)
3f	246 (0.98)	246 (1.07)	215 (3.18)	231 (1.67)	—	—
	281 (0.66)	281 (0.72)	281 (1.05)	280 (1.07)	280 (0.24)	281 (0.25)
	408 (1.15)	409 (1.23)	406 (1.06)	407 (1.10)	416 (0.42)	414 (0.41)

stituent of the furan-2-one fragment, products **3a**, **3c**, **3f** show three bands in solution (chloroform, ethanol), corresponding to the π→π* and n→π* transitions at 215–248 nm, 281–298 nm and 384–408 nm, respectively. In a DMSO solution, two bands are observed (the first band is not detected due to the lower transmission limit of DMSO) at 280–296 nm and 396–416 nm. The first two absorption bands correspond to the furan-2-one and chromen-4-one fragments. The appearance of a new absorption band in the long-wavelength region is associated with the formation of a single conjugation system, including both fragments (Figure 8).

In DMSO, due to the high basicity and dielectric constant of this solvent, which is an effective electron donor, the interaction between this solvent and (*E*)-3-((2-oxo-5-phenylfuran-3(2*H*)-ylidene)methyl)- 4*H*-chromen-4-one (**3a**) results in a significant hyperchromic band effect at 403 nm. When moving from the "parent" compound to (*E*)-3-((5-(4-chlorophenyl)-2-oxofuran-3(2*H*)-ylidene) methyl)-4*H*-chromen-4-one (**3c**) in the case of using an aprotic non-polar solvent (chloroform), there is no bathochromic shift of the band at 391 nm, but its hyperchromic effect is also observed, which is probably associated with nonspecific orientational, inductive and dispersive interactions of this solvent with the electron-withdrawing substituent (–Cl). Due to the introduction of an additional polar group (**3f**) containing a lone electron pair (–OCH_3 group), a bathochromic shift (λ = 416 nm) is observed relative to compounds **3a** and **3c**.

In the presence of catalytic amounts of glacial acetic acid in all of the above solvents, the position of the bands does not change, while the intensity of the band (hyperchromic effect) corresponding to the n→π* transition slightly increases (Table 6).

4. Conclusions

In summary, hybrid compounds based on furan-2(3*H*)-ones and chromen-4(4*H*)-one: (*E*)-3-{[2-oxo-5-arylfuran-3(2*H*)-ylidene]methyl}-4*H*-1-benzopyran-4-ones were prepared and structurally characterized. Using experimental and calculated data, they showed the probable path of transformations, the structure of the intermediates of the process and the final reaction products. The resulting hybrid compounds exist only in the *E*-configuration.

Supplementary Material

Copies of ^{1}H, ^{13}C, NOESY NMR spectra of the products are presented in the supporting information.

CCDC–2350345 contains the supplementary crystallographic data for this paper. These data can be obtained free of charge at http:// www.ccdc.cam.ac.uk/const/retrieving.html or from the Cambridge Crystallographic Data Centre (CCDC), 12 Union Road, Cambridge CB2 1EZ, UK; fax: +44(0)1223-336033 or e-mail: deposit@ccdc.cam.ac.uk.

Acknowledgement

This research was funded by Foundation for Assistance to Small Innovative Enterprises (FASIE) (grant No. 18695GU/2023 to E. M. Arzyamova).

Conflict of interest

The authors declare no conflict of interest.

5. References

1. D. V. Lipina, E. I. Denisova, I. O. Devyatkin, E. A. Okoneshnikova, D. A. Shipilovskikh, R. R. Makhmudov, N. M. Igidov, S. A. Shipilovskikh, *Russ. J. Gen. Chem.* **2021**, *91*, 2469–2474. **DOI**10.1134/S1070363221120161
2. S. N. Igidov, D. V. Lipin, A. Yu. Turyshev, S. V. Chashchina, D. A. Shipilovskikh, O. V. Zvereva, K. A. Mitusova, P. S. Silaichev, N. M. Igidov, *Chim. Techn. Acta* **2023**, *10*, 1–8. **DOI**10.15826/chimtech.2023.10.1.02
3. E. M. Flefel, W. A. Tantawy, R. E. Abdel-Mageid, A. El-Galil E. Amr, R. Nadeem, *Res. Chem. Intermed.* **2014**, *40*, 1365–1381. **DOI**10.1007/s11164-013-1045-z
4. J. P. Rappai, V. Raman, P. A. Unnikrishnan, S. Prathapan, S. K. Thomas, C. S. Paulose, *Bioorg. Med. Chem. Lett*. **2009**, *19*, 764–765. **DOI**10.1016/j.bmcl.2008.12.030
5. M. M. Alam, D. P. Sarkar, A. Husain, A. Marella, M. Shaquiquzzaman, M. Akhter, M. Shaharyar, O. Alam, F. Azam, *J. Serb. Chem. Soc.* **2011**, *76*, 1617–1626. **DOI**10.2298/JSC110131142A
6. T. Bhando, T. Bhattacharyya, A. Gaurav, J. Akhter, M. Saini, V. K. Gupta, S. K. Srivastava, H. Sen, N. K. Navani, V. Gupta, D. Biswas, R. Chaudhry, R. Pathania, *J. Antimicrob. Chemother*. **2020**, *75*, 418–428. **DOI**10.1093/jac/dkz428
7. M. S. Mohamed, K. M. Elamin, R. Alenazy, E. M. Eltayib, M. T. Idriss, N. A. A. Alhudaib, T. Elsaman, M. A. Mohamed, *J. Chem.* **2023**, *2023*, 1–13. **DOI**10.1155/2023/1481595
8. S. Emami, N. Shahrokhirad, A. Foroumadi, M. A. Faramarzi, N. Samadi, N. Soltani-Ghofrani, *Med. Chem. Res.* **2013**, *22*, 5940–5947. **DOI**10.1007/s00044-013-0581-9
9. A. Kamal, S. M. Ali Hussaini, S. Faazil, Y. Poornachandra, G. N. Reddy, C. G. Kumar, V. S. Rajput, C. Rani, R. Sharma, I. Ali Khan, N. J. Babu, *Bioorg. Med. Chem. Lett*. **2013**, *23*, 6842–6846. **DOI**10.1016/j.bmcl.2013.10.010
10. S. Jiang, S. Su, M. Chen, F. Peng, Q. Zhou, T. Liu, L. Liu, W. Xue, *J. Agric. Food Chem.* **2020**, *68*, 5641–5647. **DOI**10.1021/acs.jafc.0c01652
11. A. Kurt-Kızıldoğan, N. Akarsu, Ç. Otur, A. Kivrak, N. Aslan-Ertas, S. Arslan, D. Mutlu, M. Konus, C. Yılmaz, D. Cetin, T. Topal, N. Şahin, *Anticancer Agents Med. Chem.* **2022**, *22*, 362–370. **DOI**10.2174/1871520621666210311085748

12. F. Peng, T. Liu, Q. Wang, F. Liu, X. Cao, J. Yang, L. Liu, C. Xie, W. Xue, *J. Agric. Food Chem.* **2021**, *69*, 11085–11094. **DOI**10.1021/acs.jafc.1c03755
13. A. A. El-Tombary, Y. S. Abdel-Ghany, A. S. F. Belal, S. A. S. El-Dine, F. S. G. Soliman, *Med. Chem. Res.* **2011**, *20*, 865–876. **DOI**10.1007/s00044-010-9394-2
14. R. Zhang, G. Iskander, P. Da Silva, D. Chan, V. Vignevich, V. Nguyen, M. M. Bhadbhade, D. StC Black, N. Kumar, *Tetrahedron* **2011**, *67*, 3010–3016. **DOI**10.1016/j.tet.2011.02.014
15. Y. Isyaku, A. Uzairu, S. Uba, M. T. Ibrahim, A. B. Umar, *Bull. Nat. Res. Centre* **2020**, *44*, 1–11. **DOI**10.1186/s42269-020-00297-w
16. F. Hao, X. Wang, M. Mohammadnia, *Polycycl. Aromat. Compd.* **2022**, *42*, 4255–4269. **DOI**10.1080/10406638.2021.1887298
17. H. Shahbazi-Alavi, S. Khojasteh-Khosro, J. Safaei-Ghomi, S. H. Nazemzadeh, *J. Iran. Chem. Soc.* **2019**, *16*, 2433–2440. **DOI**10.1007/s13738-019-01711-5
18. A. K. El-Ziaty, W. S. I. Abou-Elmagd, S. K. Ramadan, A. I. Hashem, *Egypt. J. Chem.* **2016**, *59*, 637–646.
19. S. E. Denmark, B. R. Henke, *J. Am. Chem. Soc.* **1991**, *113*, 2177–2194. **DOI**10.1021/ja00006a042
20. OD Rigaku (2022). *CrysAlis PRO*. Rigaku Oxford Diffraction, Yarnton, Oxfordshire, England.
21. G. M. Sheldrick, *Acta Crystallogr.* **2015**, *C71*, 3–8. **DOI**10.1107/S2053229614024218
22. O. V. Dolomanov, L. J. Bourhis, R. J. Gildea, J. A. K. Howard, H. Puschmann, *J. Appl. Crystallogr.* **2009**, *42*, 339–341. **DOI**10.1107/S0021889808042726
23. V. A. Sedavkina, N. A. Morozova, A. Yu. Egorova, I. G. Ostroumov, *Chem. Heterocycl. Compd.* **1987**, *23*, 377–380. **DOI**10.1007/BF00546727

Povzetek

Razvili smo direktno metodo priprave hibridnih spojin (*E*)-3-{[2-okso-5-arilfuran-3(2*H*)-iliden]metil}-4*H*-1-benzopiran-4-onov, ki temeljijo na furan-2(3*H*)-onu in kromen-4(4*H*)-onu. Strukture smo potrdili z elementno analizo, IR, UV in NMR spektroskopijo ter z rentgensko difrakcijo monokristala. Molekulsko geomterijo sintetizirane spojine (*E*)-3-((2-okso-5-fenilfuran-3(2*H*)-iliden)metil)-4*H*-kromen-4-ona (**3a**) smo analizirali z rentgensko difrakcijsko analizo ter rezultate primerjali z rezultati DFT izračunov, izvedenih s 6-311G bazno funkcijo z razcepljenimi valencami.